Electronically and Orthogonally Tunable SITO Voltage-Mode Multifunction Biquad Filter Using LT1228s

May Phu Pwint Wai, Peerawut Suwanjan, Winai Jaikla*, Amornchai Chaichana
Department of Engineering Education, School of Industrial Education and Technology,
King Mongkut's Institute of Technology Ladkrabang,
10520 Bangkok, Thailand
winai.ja@kmitl.ac.th

***Abstract*—The commercially available IC LT1228 is an interesting active device due to its advantage features, such as a fast transconductance amplifier, a wide bandwidth over a wide range of voltage gain, low total harmonic distortion (THD), high impedance differential input, etc. The single-input triple-output (SITO) voltage-mode (VM) multifunction biquadratic filters using ICs, LT1228s are introduced in this research. This circuit design provides the three-filtering functions, low-pass (LP), high-pass (HP), and band-pass (BP), without changing the circuit architecture. It comprises three LT1228s, four resistors, and two capacitors connected to the ground. The low impedance voltage output nodes are HP and BP responses. The quality factor (Q) and the pole frequency (ω_0) can be electronically and orthogonally tuned by altering the third LT1228's bias current (I_B). The PSPICE simulation and the experiment are verified to describe the circuit operation.**

***Index Terms*—LT1228; Voltage-mode; SITO; Biquadratic filter; Active building block.**

I. INTRODUCTION

The realization of a continuous-time filter utilizing the electronically adjustable active building block (ABB) has been mainly focused on the research topic due to its advantages, e.g., it gives better adjustment than varying the value of the passive device. It is a significant building block of analog signal processing, automatic control, and instrumentation systems, such as touch-tone telephone systems, three-way crossover networks, digital television (DTV), and phased locked loop circuits. A circuit simultaneously provides LP, HP, and BP filters are always used in the electrical and electronics engineering field, such as the three-way crossover network [1]–[3].

The current feedback amplifier (CFA) has drawn in extensive regard for design superior performance electronic circuits. CFA is essentially a current mode device and is utilized in high-frequency operations. Moreover, it gives faster slew rates, lower distortion, very high full-power bandwidth, and provides a large output current drive capability. Numerous commercial CFA ICs are accessible, e.g., AD844 CFA using the macro model available from Analog Devices, AD8011 from Analog Devices [4], [5]. The LT1228 integrated circuit by Linear Technology is one of the intriguing elements [6]. It comprises two independent sub-elements: the operational transconductance amplifier (OTA), whose transconductance (g_m) can be electronically controlled by bias current and the CFA which can be used as a voltage buffer or amplifier.

The voltage-mode multifunction biquadratic filters using ABB implemented from the commercially available ICs have been recently published in [7]–[19]. The biquad multifunction filters utilizing LT1228 as an active element were proposed in [12], [13], [15], [16]. The ABB employed [8]–[10] is constructed from the different commercially available ICs. Some filters proposed in [10], [14], [18] don't use the grounded capacitors. The biquad filter in [18] is not provided the low output impedance. As a result, it requires the buffer to connect the other circuits. Both ω_0 and Q of the proposed filters in [7], [9], [11], [14], [18] cannot be offered electronic controllability, while the circuits proposed in [8], [10], [12], [14], [17], [18] cannot be independently tuned.

An electronically and orthogonally controllable SITO VM multifunction biquadratic filtering circuit using LT1228 as an active building block is proposed in this paper. This circuit can orthogonally and electronically control the filtering parameters, the ω_0 and Q. It gives low output impedances at HP and BP responses, so it can be directly cascaded to other circuits. This filter uses the grounded capacitors being attractable for the cancellation of non-ideal effects of LT1228. To affirm the circuit performance of the presented filter, the PSPICE simulation utilizing the LT1228 and theoretical results are described.

II. PRINCIPLE OF OPERATION

The schematic symbol, equivalent circuit, and block diagram of LT1228 are illustrated in Fig. 1(a), Fig. 1(b), and Fig. 1(c). The LT1228 OTA has a current source with high output impedance Pin 1) and a differential voltage with high input impedance (Pin 2 and Pin 3). Pins 4 and 7 are the positive and negative supply voltages. The transconductance, g_m, is controlled by the current that flows into Pin 5, I_B. The CFA's non-inverting input is designed to drive the voltage terminals with low output impedance (Pin

Manuscript received 27 February, 2021; accepted 19 June, 2021.
This research was supported by King Mongkut's Institute of Technology Ladkrabang (KMITL).

6) to give the excellent linearity at high frequencies. Pin 8 is the inverting input of CFA and it has a low impedance.

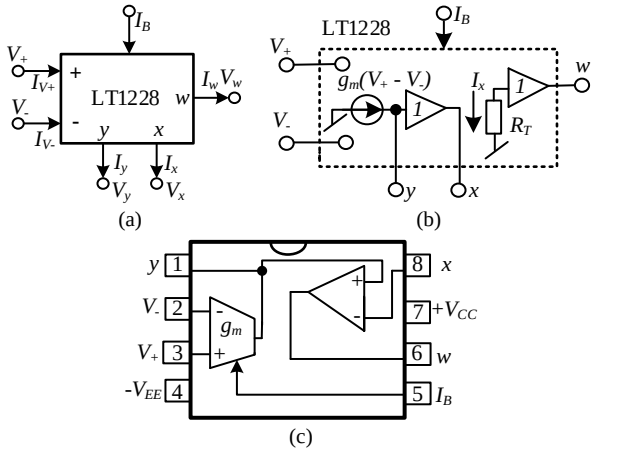

Fig. 1. (a) Schematic representation; (b) Equivalent circuit; (c) Block diagram.

The ideal property of LT1228 is expressed in (1):

$$\begin{pmatrix} I_{V+} \\ I_{V-} \\ I_y \\ V_x \\ V_w \end{pmatrix} = \begin{pmatrix} 0 & 0 & 0 & 0 & 0 \\ 0 & 0 & 0 & 0 & 0 \\ g_m & -g_m & 0 & 0 & 0 \\ 0 & 0 & 1 & 0 & 0 \\ 0 & 0 & 0 & R_T & 0 \end{pmatrix} \begin{pmatrix} V_+ \\ V_- \\ V_y \\ I_x \\ I_w \end{pmatrix}, \tag{1}$$

where R_T is the trans-resistance gain. In an ideal case, R_T approaches infinity. The transconductance g_m of LT1228 can be described as follows

$$g_m = I_B / 3.87V_T, \tag{2}$$

where I_B is the DC bias current and V_T is the thermal voltage. It reveals from (2) that the g_m is electronically controlled by bias current I_B, which is required for the modern circuit. However, the g_m is inversely proportional to temperature.

III. Synthesis of Multifunction Filter

The proposed filter is synthesized from the block diagram in Fig. 2. It consists of five basic blocks: the voltage summing circuit, two lossless integrators, and two voltage amplifiers. The inputs of the voltage summing circuit are V_{LP}, V_{BP}, and V_{in}, while the output voltage node of the summing circuit is V_{HP}. The voltage node, V_{BP}, is the output of the first lossless integrator multiplied by the voltage gain amplifier, K. The V_{LP} is the output of the second lossless integrator. The time constant of the first and the second integrators are defined as a and b, respectively.

The three voltage transfer functions for V_{HP}, V_{BP}, and V_{LP} of the block diagram shown in Fig. 2 are respectively obtained as:

$$\frac{V_{LP}}{V_{in}} = \frac{\frac{1}{ab}}{s^2 + \frac{sK}{a} + \frac{3}{ab}}, \tag{3}$$

$$\frac{V_{HP}}{V_{in}} = \frac{-s^2}{s^2 + \frac{sK}{a} + \frac{3}{ab}}, \tag{4}$$

$$\frac{V_{BP}}{V_{in}} = \frac{-\frac{sK}{a}}{s^2 + \frac{sK}{a} + \frac{3}{ab}}. \tag{5}$$

Equations (3)–(5) indicate that the unity passband voltage gain is obtained for the BP and HP functions and one-third passband voltage-gain is obtained for the LP function. The ω_0 and Q are respectively obtained as

$$\omega_0 = \sqrt{\frac{3}{ab}}, \tag{6}$$

$$Q = \frac{1}{K}\sqrt{\frac{3a}{b}}. \tag{7}$$

Equations (6) and (7) shows that the Q can be adjusted without disturbing the ω_0 by varying the voltage gain, K. Simultaneously adjusting the time constants a and b of the integrator circuits can control the ω_0 without affecting the Q. Then ω_0 and Q are independently controlled, where the Q can be adjusted by the voltage gain, K, and the ω_0 can be linearly adjusted by the time constants of both integrators.

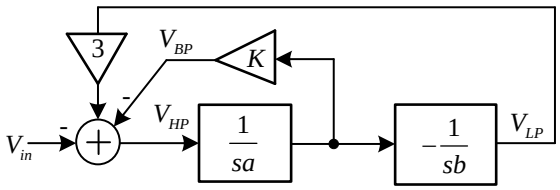

Fig. 2. Synthesis block diagram of the proposed voltage-mode multifunction filter.

IV. Proposed Multifunction Filter

The proposed multifunction filter is shown in Fig. 3. It consists of three LT1228s, four resistors, and two grounded capacitors. The filter in Fig. 3 is synthesized from the block diagram in Fig. 2.

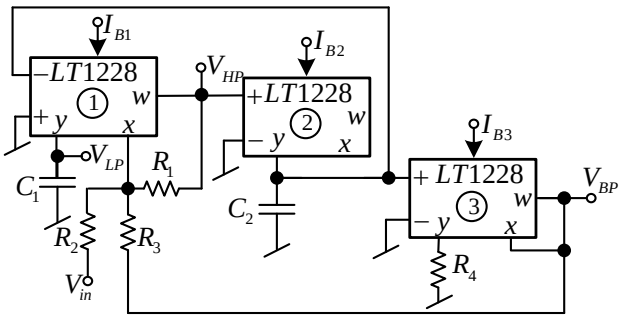

Fig. 3. Proposed SITO voltage-mode multifunction filter.

The capacitor C_1 and the first LT1228 are constructed as the first lossless integrator, while the capacitor C_2 and the second LT1228 are built as a second lossless integrator. The voltage summing circuit is constructed from the resistors R_1, R_2, and R_3 (they are same resistance value) and the first

LT1228. Finally, the amplifier consists of the resistor R_4 and the third LT1228. The single input voltage, V_{in}, is applied at the voltage summing circuit, while the first integrator produces the low-pass filtering output voltage node, V_{LP}, the voltage summing produces the high-pass filtering output voltage node, V_{HP}, and the voltage amplifier produces the band-pass filtering output voltage node, V_{BP}. With this design, three voltage mode second-order filtering functions are simultaneously given without changing the filtering architecture. Moreover, the proposed filter provides the low output impedance at output voltage nodes V_{HP} and V_{BP}. These voltage transfer functions of the proposed circuit are given by:

$$\frac{V_{LP}}{V_{in}} = \frac{\frac{g_{m1}g_{m2}}{C_1C_2}}{s^2 + \frac{sg_{m3}R_4g_{m2}}{C_2} + \frac{3g_{m1}g_{m2}}{C_1C_2}}, \tag{8}$$

$$\frac{V_{BP}}{V_{in}} = \frac{-\frac{sg_{m3}R_4g_{m2}}{C_2}}{s^2 + \frac{sg_{m3}R_4g_{m2}}{C_2} + \frac{3g_{m1}g_{m2}}{C_1C_2}}, \tag{9}$$

$$\frac{V_{HP}}{V_{in}} = \frac{-s^2}{s^2 + \frac{sg_{m3}R_4g_{m2}}{C_2} + \frac{3g_{m1}g_{m2}}{C_1C_2}}. \tag{10}$$

From (8)–(10), the high-pass and band-pass functions are obtained unity passband voltage gain, while the low-pass function is also obtained one-third passband voltage gain. In addition, from them, the inverting for the high-pass and band-pass functions is achieved and the non-inverting for the low-pass response is achieved. The ω_0 and Q are described as follows:

$$\omega_0 = \sqrt{\frac{3g_{m1}g_{m2}}{C_1C_2}}, \tag{11}$$

$$Q = \frac{1}{g_{m3}R_4}\sqrt{\frac{3g_{m1}C_2}{g_{m2}C_1}}. \tag{12}$$

Substituting the I_{B1}, I_{B2}, and I_{B3} from (2) into transconductances g_{m1}, g_{m2}, and g_{m3} to (11) and (12), the ω_0 and Q of the proposed filter are as follows:

$$\omega_0 = \frac{1}{3.87V_T}\sqrt{\frac{3I_{B1}I_{B2}}{C_1C_2}}, \tag{13}$$

$$Q = \frac{1}{I_{B3}R_4}\sqrt{\frac{3I_{B1}C_2}{I_{B2}C_1}}. \tag{14}$$

From (13) and (14), it can be seen that ω_0 can be electronically tuned by I_{B1} and I_{B2}. Moreover, the Q can be altered without disturbing ω_0 by changing the value of I_{B3}. If the bias currents $I_{B1} = I_{B2} = I_B$ (this property is easily implemented by using a microcontroller or microcomputer) are simultaneously adjusted and choosing $C_1 = C_2 = C$, the filtering parameters in (11) become

$$\omega_{01} = \frac{I_B}{3.87V_TC}\sqrt{3}, \tag{15}$$

$$Q = \frac{\sqrt{3}}{I_{B3}R_4}. \tag{16}$$

It can be remarked from (15) and (16) that ω_0 and Q are independently, electronically controlled. Moreover, the ω_0 and Q can be linearly and electronically adjusted.

V. PARASITIC EFFECT ON LT1228

In real response, the parasitic elements of LT1228 affect the performance of the circuit, so they are described in detail in this section. These parasitic elements are grounded passive elements (resistors and capacitors) at high impedance V_+, V_-, and y terminal. They can be characterized as R_+, C_+, R_-, C_-, R_y, and C_y, respectively. The impedance terminals x and w show up in the arrangement resistors R_x and R_w individually since these terminals have low impedance. The trans-resistance gain R_T is paralleled by C_T. According to the data sheet of LT1228 [6], to reduce the effect of C_T and R_T and to get higher operating frequency, the feedback resistor (R_1 in this filter) connecting from w to x terminal in the summing circuit should be low. In addition, if the bandwidth of the presented filter is expected to be lower than 10 MHz, the greatest effect stems from R_-, C_-, R_+, C_+, R_y, and C_y . So, the effect of R_x, R_w, R_T, and C_T is ignored. Moreover, if the operational frequency of the presented filter is expected to be lower than G_{y3}^*/C_{y3}, the effect of C_{y3} is also ignored. Considering these parasitic elements, the voltage transfer functions of the proposed filter are as follow:

$$\frac{V_{LP}}{V_{in}} = \frac{\frac{g_{m1}g_{m2}}{C_1^*C_2^*}}{D(s)}, \tag{17}$$

$$\frac{V_{BP}}{V_{in}} = \frac{-\frac{K^*g_{m2}G_{y1}}{C_1^*C_2^*} - \frac{K^*g_{m2}}{C_2^*}s}{D(s)}, \tag{18}$$

$$\frac{V_{HP}}{V_{in}} = \frac{-s^2 - \left(\frac{G_{y1}C_2^* + G_{y2}^*C_1^*}{C_1^*C_2^*}\right)s - \frac{G_{y1}G_{y2}^*}{C_1^*C_2^*}}{D(s)}, \tag{19}$$

where

$$D(s) = \begin{bmatrix} s^2 + \left(\frac{G_{y1}C_2^* + G_{y2}^*C_1^* + K^*g_{m2}C_1^*}{C_1^*C_2^*}\right)s + \\ \frac{G_{y1}G_{y2}^* + 3g_{m1}g_{m2} + K^*g_{m2}G_{y1}}{C_1^*C_2^*} \end{bmatrix}, \tag{20}$$

and $K^* = \frac{g_{m3}}{G_{y3}^*}$, $C_1^* = C_1 + C_{y1}$, $C_2^* = C_2 + C_{y2} + C_{-1} + C_{+3}$,

$G_{y1} = \frac{1}{R_{y1}}$, $G_{y2}^* = \frac{1}{R_{y2}} + \frac{1}{R_{+3}} + \frac{1}{R_{-1}}$, and $G_{y3}^* = \frac{1}{R_{y3}} + \frac{1}{R_4}$.

From (20), the non-ideal factors of the natural frequency and quality are given by:

$$\omega_0^* = \sqrt{\frac{G_{y1}G_{y2}^* + K^* g_{m2}G_{y1} + 3g_{m1}g_{m2}}{C_1^* C_2^*}}, \quad (21)$$

$$Q^* = \frac{1}{\frac{G_{y1}}{C_1^*} + \frac{G_{y2}^*}{C_2^*} + \frac{K^* g_{m2}}{C_2^*}} \sqrt{\frac{G_{y1}G_{y2}^* + K^* g_{m2}G_{y1} + 3g_{m1}g_{m2}}{C_1^* C_2^*}}. \quad (22)$$

It is seen from (17) to (22) that the parasitic elements in LT1228 affect the filtering performances which are the operational frequency, passband voltage gain, natural frequency, and quality factor.

VI. Simulation Results

The functionality of the presented filter has been matched with the LT1228 PSPICE macro model simulation. In this simulation, the symmetrical supply voltages are ± 5 VDC, the components are chosen as follows: $I_{B1} = I_{B2} = I_{B3} =$ 100 µA, $R_1 = R_2 = R_3 = R_4 =$ 1 kΩ, and $C_1 = C_2 =$ 2.7 nF. The f_0 and Q from (15), (16) are obtained as 102.097 kHz and 1.732, respectively. The magnitude of LP, HP, and BP versus frequency of the proposed voltage-mode multifunction biquadratic filter is shown in Fig. 4. The simulated f_0 is 100.46 kHz and Q is 1.71. The percent deviations of the expected and simulated values of Q and f_o are 1.27 % and 1.6 %, respectively. Figure 5 shows the HP frequency response with different values of R ($R_1 = R_2 = R_3 = R$), where the values of R in the summing circuit are set to 0.2 kΩ, 0.6 kΩ, and 5 kΩ. It is verified that the bandwidth at the low value of the feedback resistor (R_1) in the proposed filter is higher than the bandwidth at the high value of R_1 as described in the parasitic section. Thus, these resistors are chosen as 1 kΩ to achieve higher operational frequency. Figure 6 indicates the test of the transient response of the presented voltage-mode band-pass filter where the sinusoidal input voltage is applied to 50 mV_p and $f_0 =$ 100 kHz.

The Q value is controlled without disturbing the f_0 as shown in Fig. 7. It is verified that Q can be orthogonally controlled by simultaneously adjusting the DC bias current, I_{B3}, to 123.5 µA, 185.5 µA, and 371 µA. Figure 8 confirms that Q can be controlled by varying the value of resistance R_4 without affecting f_0 as expected in (15), (16), where R_4 is assigned to 1 kΩ, 2 kΩ, and 3 kΩ. The control of the pole frequency can be electronically tuned by simultaneously varying the values of I_{B1} and I_{B2} as described in (15), (16). This adjustment of I_{B1} and I_{B2} is easily implemented by using a microcontroller or microcomputer. This is verified by the simulated results in Fig. 9. The BP responses are simulated for three different values, where f_0 is set to 123.311 kHz, 185.353 kHz, and 373.25 kHz at the same value of Q = 1.6. The simulation results of the total harmonic distortion (THD) versus the magnitude of the input voltage are illustrated in Fig. 10. The input linear range of the proposed filter is around 50 mV_p because the internal construction of LT1228 is BJT OTA.

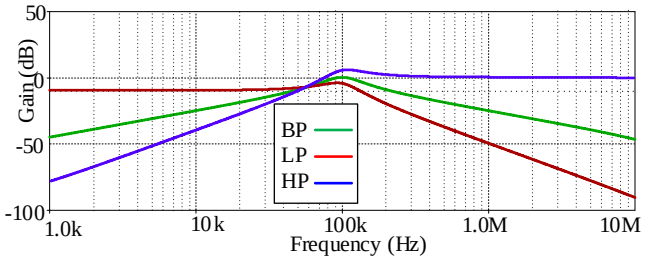

Fig. 4. Magnitude responses of BP, LP, and HP.

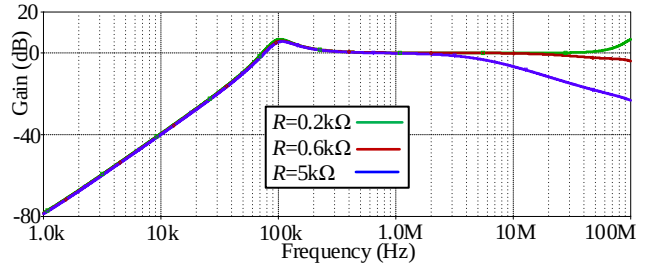

Fig. 5. Simulated HP frequency responses of the biquadratic filter with different values of R ($R_1 = R_2 = R_3 = R$).

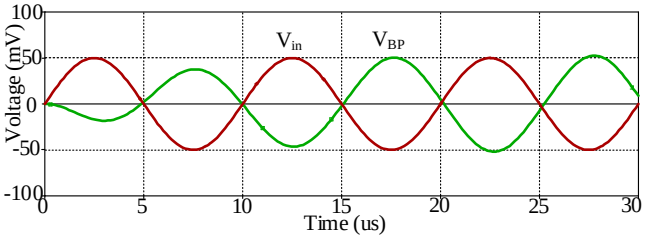

Fig. 6. Time-domain responses of the presented BP function.

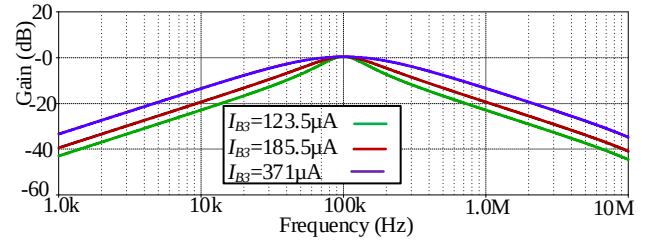

Fig. 7. Simulated BP frequency responses for different values of I_{B3}.

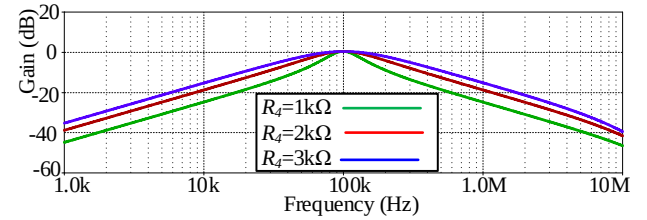

Fig. 8. Simulated BP frequency responses for different values of R_4.

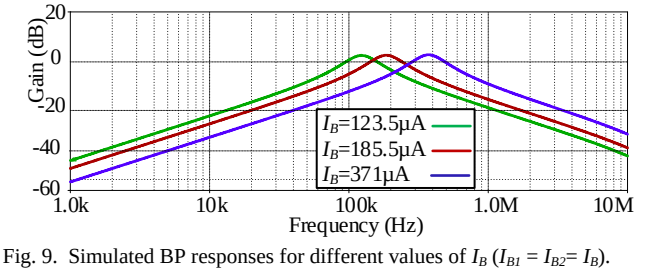

Fig. 9. Simulated BP responses for different values of I_B ($I_{B1} = I_{B2} = I_B$).

The 10 mV_p of the sinusoidal input voltage signal is applied with three frequencies, such as 10 kHz, 100 kHz, and 1 MHz. The input and the output voltage signals for the BP frequency spectrum result are demonstrated in Fig. 11. It

is found that the attenuation between the pole frequency (100 kHz) and f = 10 kHz is -25.52 dB, while the attenuation between the pole frequency (100 kHz) and f = 1 MHz is -5.82 dB.

The simulation results in Figs. 6–11 indicate that the proposed filter operates well as expected. The operational frequency is around 10 MHz. The total harmonic distortion is lower than 1 % when the applied amplitude of the input signal is lower than 50 mV_p.

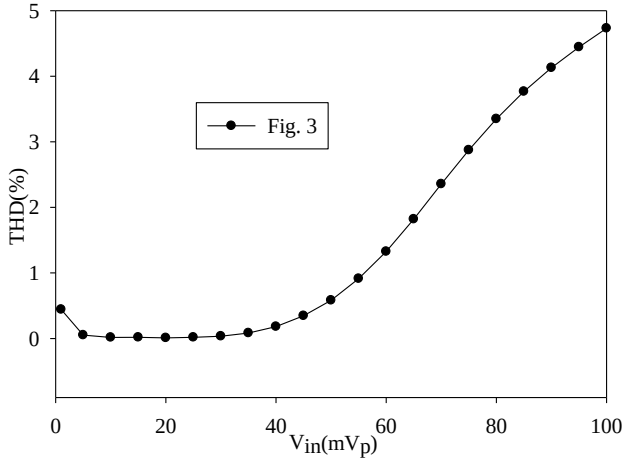

Fig. 10. THD test of the BP versus input voltage amplitude.

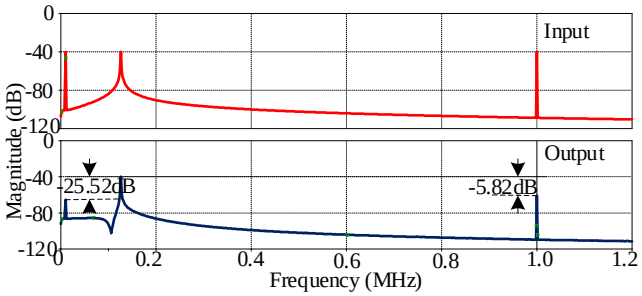

Fig. 11. The desirable test signal of the BP.

VII. EXPERIMENTAL RESULTS

To verify the performance of the proposed biquadratic multifunction filtering design in Fig. 3, the tests are made by using three LT1228s. The power supply voltage is ±5 V using GW Instek GPS-3303 power supply. In the experiment, the components are selected: $C_1 = C_2$ = 2.7 nF, $R_1 = R_2 = R_3 = R_4$ = 1 kΩ, and $I_{B1} = I_{B2} = I_{B3}$ =100 µA. The calculated pole frequency and the quality factor are f_0 = 102.097 kHz and Q = 1.732, respectively. The sinusoidal input signal and the output waveforms are measured by the Keysight DSOX1102G oscilloscope. Figure 12 illustrates the experimental and theoretical results of the filter with the input voltage amplitude being 50 mV_{p-p} to keep LT1228 operating in linear range. The experimental pole frequency is f_0 = 100 kHz. Due to the parasitic elements of LT1228, the experimental results slightly deviate from the ideal results at low-frequency, and tolerances of the parasitic capacitance effect at high frequency (higher 10 MHz). Next, the transient response of the BP filtering function is also investigated by applying a 50 mV_{p-p} sinusoidal input voltage for the three frequencies (50 kHz, 100 kHz, and 500 kHz) shown in Fig. 13. It is found that at low (50 kHz) and high frequency (500 kHz), the output voltages are attended, while at natural frequency (100 k), the input and the output voltages are the same magnitude. Figure 14 shows the magnitude response of the band-pass filter at different I_{B3} values (123.5 µA, 185.5 µA, and 371 µA). It is verified that the pole frequency is linearly and electronically tuned by I_{B3} without affecting the Q as expected in (15), (16). To keep the f_0 value constant at 100 kHz by varying the resistor R_4, the adjustment of the Q value is verified in Fig. 15. The band-pass responses for the three different values of f_0 at Q = 1.6 can be obtained by simultaneously varying the values of the bias currents, I_{B1} and I_{B2} (where the three different values of these bias currents are 123.5 µA, 185.5 µA, and 371 µA). In practical, this adjustment of I_{B1} and I_{B2} is easily implemented by using a microcontroller. This result is demonstrated in Fig. 16.

The experimental results in Figs. 12–16 indicate that the proposed filter operates well as expected. However, at high frequency, the parasitic capacitances in LT1228 will affect the performance of the proposed filter as results in Fig. 12, Figs. 14–16.

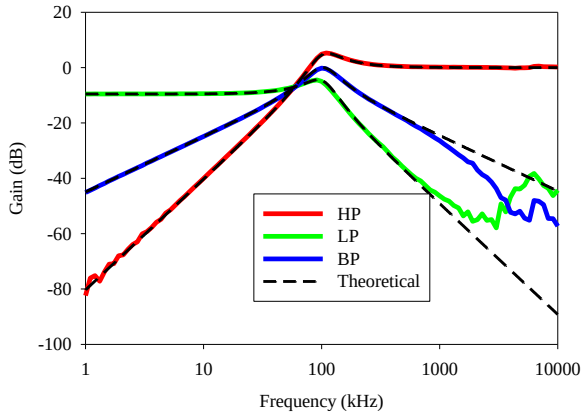

Fig. 12. The experimental frequency response of the filter.

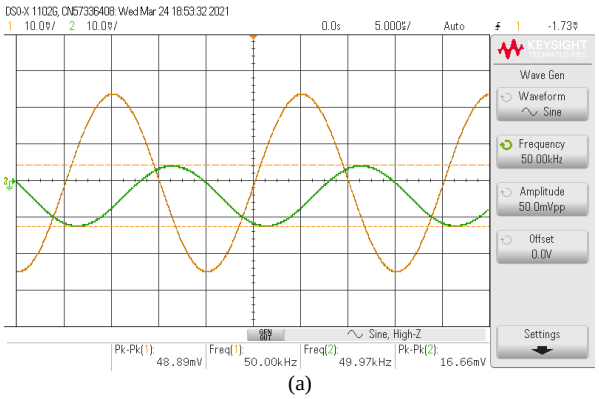

(a)

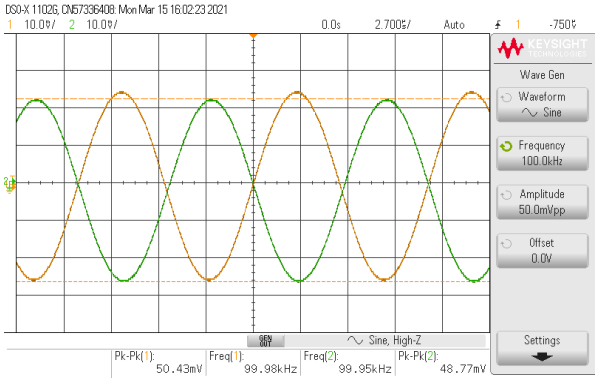

(b)

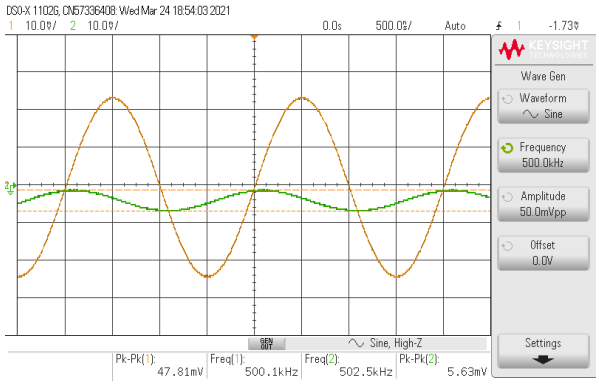

(c)

Fig. 13. The transient response of the proposed SITO BP function (orange line is the input and green line is the output): (a) f = 50 kHz, (b) f = 100 kHz, (c) f = 500 kHz.

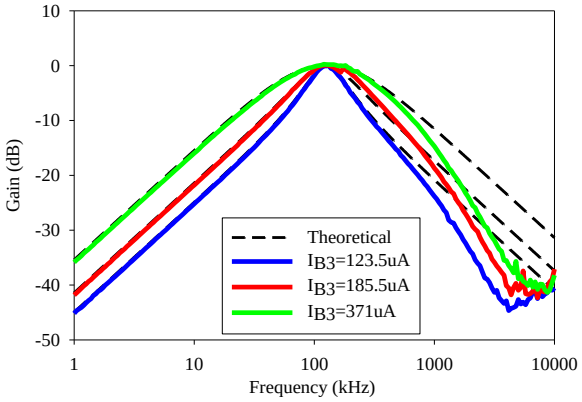

Fig. 14. The experimental response of BP for different values of I_{B3}.

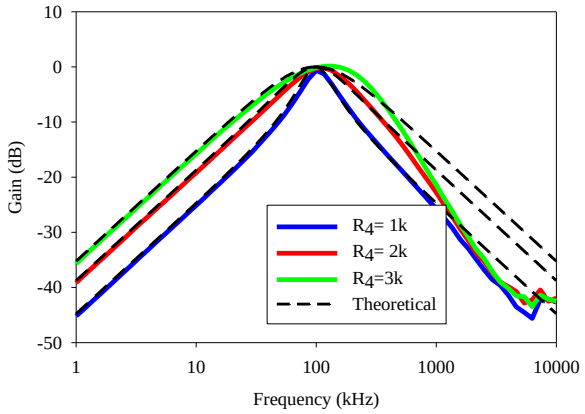

Fig. 15. The experimental response of BP for different values of R_4.

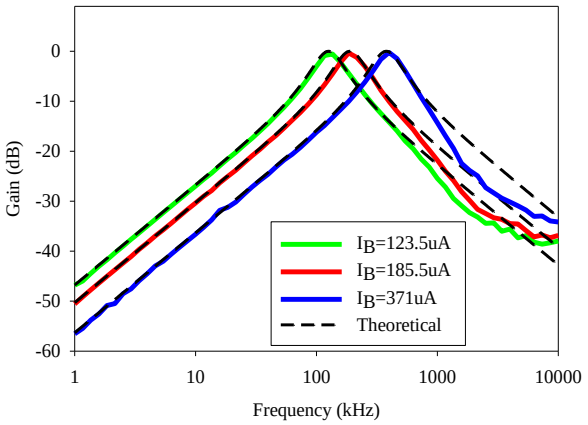

Fig. 16. The experimental response of BP for different values of I_B.

VIII. COMPARISON AND DISCUSSION

Table I compares the proposed multifunction biquad filter with recent biquad filters using ABBs implemented from the commercially available ICs [7]–[18]. The proposed filter and the circuits in [9], [12] are single input multiple output. The biquad filters in [7], [9], [11], [13], [15]–[17] are multiple input multiple output, and the filters in [8], [10], [14], [18] are multiple input single output configuration. The biquad multifunction filters in [8]–[10] are constructed from the different commercially available ICs. The filters in [15], [16] consist of five LT1228s.

TABLE I. COMPARISON OF THE PROPOSED MULTIFUNCTION FILTER AND RECENT BIQUAD FILTERS USING ABBs.

Ref.	ABB	No. of commercial ICs	All grounded C	Providing several functions at the same time	Filtering functions	No. of low Z_o nodes	Electronic tune both f_0 and Q	Independent tune of f_0 and Q	Voltage supplies
[7]	AD844	3	Yes	No	LP, HP, BP	3	No	Yes	±6 V
[8]	VDDDA	4	Yes	No	LP, HP, BP, BR, AP	1	Yes	No	±5 V
[9]	VD-DIBA	4	Yes	Yes	LP, HP, BP, BR, AP	2	No	Yes	±5 V
[10]	VDBA	4	No	No	LP, HP, BP, BR, AP	1	Yes	No	±5 V
[11]	AD844	3	Yes	Yes	LP, BP, BR	3	No	Yes	±6 V
[12]	LT1228	2	Yes	Yes	LP, BP, HP	2	Yes	No	±5 V
[13]	LT1228	4	Yes	Yes	LP, BP, BR	3	Yes	Yes	±15 V
[14]	AD844	3	No	No	LP, BP, HP, BR, AP	1	No	No	±6 V
[15]	LT1228	5	Yes	Yes	LP, BP, HP, BR, AP	3	Yes	Yes	±15 V
[16]	LT1228	5	Yes	Yes	LP, BP, HP, BR, AP	3	Yes	Yes	±15 V
[17]	AD844	3	Yes	Yes	LP, BP, HP, BR	3	No	No	±6 V
[18]	FTFN	2	No	No	LP, BP, HP, BR, AP	0	No	No	±10 V
This work	LT1228	3	Yes	Yes	LP, BP, HP	2	Yes	Yes	±5 V

Notes: VDDDA and VD-DIBA are constructed from two commercially available ICs, LM13700 and AD830; VDBA is constructed from two commercially available ICs, CA3080 and LF356; FTFN is constructed from two commercially available ICs, AD844.

In [10], [14], [18], these filters employ the floating capacitor, while the proposed filter uses grounded capacitors which ensure the compensation of the parasitic effects in ABB. The filters in [7], [8], [10], [14], [18] cannot simultaneously provide several filter responses. Although the proposed filter provides only LP, HP, and BP responses, but it is sufficient to be applied in some applications, such as the three-way crossover network. The biquad filter in [18] does not provide the low output impedance. As a result, it requires the buffer to connect the other circuits. Both ω_0 and Q of the proposed filter in [7], [9], [11], [14], [18] cannot be offered electronic controllability which is not suitable for modern circuits which are controlled by microcontroller or microprocessor. The ω_0 and Q of the filters proposed in [8], [10], [12], [14], [17], [18] cannot be independently tuned.

IX. CONCLUSIONS

In this work, an electronically and independently controllable SITO voltage-mode multifunction biquadratic filtering circuit is proposed. The proposed filter consists of triple LT1228s, two grounded capacitors, and four resistors. This proposed filter capable of producing three transfer functions, such as LP, HP, and BP, is suitable to be used in the three-way crossover network. HP and BP responses gives low output impedance is the advantage of this filter because it can be directly cascaded to other circuits without using the additional buffer. Moreover, the quality factor and the pole frequency can be independently and electronically controlled. The quality factor can be controlled by altering the third LT1228's external DC bias current value without affecting the ω_0. The simulation and experimental results are achieved to verify the theoretical analysis. The operational frequency range is lower than 10 MHz. The total harmonic distortion is lower than 1 % when the applied amplitude of the input signal is lower than 50 mV_p.

CONFLICTS OF INTEREST

The authors declare that they have no conflicts of interest.

REFERENCES

[1] A. S. Sedra and K. C. Smith, *Microelectronic Circuits*. Floida: Holt, Rinehart and Winston, 2003.

[2] A. Chaichana, S. Siripongdee, and W. Jaikla, "Electronically adjustable voltage mode first-order allpass filter using single commercially available IC", *IOP Conference Series: Materials Science and Engineering*, vol. 559, no. 1, p. 012009, 2019. DOI: 10.1088/1757-899X/559/1/012009.

[3] L. Safari, G. Barile, G. Ferri, and V. Stornelli, "High performance voltage output filter realizations using second generation voltage conveyor", *International Journal of RF and Microwave Computer-Aided Engineering*, vol. 28, no. 9, 2018. DOI: 10.1002/mmce.21534.

[4] Analog Devices, 60 MHz, 2000 V/μs, Monolithic Op Amp with Quad Low Noise, Data Sheet AD844. [Online]. Available: https://www.analog.com/media/en/technical-documentation/data-sheets/AD844.pdf

[5] Analog Devices, 300 MHz Current Feedback Amplifier, Data Sheet AD8011. [Online]. Available: https://www.analog.com/media/en/technical-documentation/data-sheets/AD8011.pdf

[6] Linear Technology, 100MHz Current Feedback Amplifier with DC Gain Control. [Online]. Available: https://www.analog.com/media/en/technical-documentation/data-sheets/1228fd.pdf

[7] S.-F. Wang, H.-P. Chen, Y. Ku, and M.-X. Zhong, "Analytical synthesis of high-pass, band-pass and low-pass biquadratic filters and its quadrature oscillator application using current-feedback operational amplifiers", *IEEE Access*, vol. 9, pp. 13330–13343, 2021. DOI: 10.1109/ACCESS.2021.3050751.

[8] W. Jaikla, F. Khateb, T. Kulej, and K. Pitaksuttayaprot, "Universal filter based on compact CMOS structure of VDDDA", *Sensors*, vol. 21, no. 5, p. 1683, 2021. DOI: 10.3390/s21051683.

[9] W. Jaikla, S. Siripongdee, F. Khateb, R. Sotner, P. Silapan, P. Suwanjan, and A. Chaichana, "Synthesis of biquad filters using two VD-DIBAs with independent control of quality factor and natural frequency", *AEU - International Journal of Electronics and Communications*, vol. 132, 2021. DOI: 10.1016/j.aeue.2020.153601.

[10] N. Roongmuanpha, T. Pukkalanun, and W. Tangsrirat, "Practical realization of electronically adjustable universal filter using commercially available IC-based VDBA", *Engineering Review*, vol. 41, 2021. DOI: 10.30765/ER.1547.

[11] S.-F. Wang, H.-P. Chen, Y. Ku, and M.-X. Zhong, "Voltage-mode multifunction biquad filter and its application as fully-uncoupled quadrature oscillator based on current-feedback operational amplifiers", *Sensors*, vol. 20, no. 22, p. 6681, 2020. DOI: 10.3390/s20226681.

[12] M. P. Pwint Wai, W. Jaikla, P. Suwanjan, and W. Sunthonkanokpong, "Single input multiple output voltage mode universal filters with electronic controllability using commercially available ICs", in *Proc. of 17th International Conference on Electrical Engineering/Electronics, Computer, Telecommunications and Information Technology*, 2020, pp. 607–610. DOI: 10.1109/ECTI-CON49241.2020.9158223.

[13] S.-F. Wang, H.-P. Chen, Y. Ku, and C.-L. Lee, "Versatile voltage-mode biquadratic filter and quadrature oscillator using four OTAs and two grounded capacitors", *Electronics*, vol. 9, no. 9, p. 1493, 2020. DOI: 10.3390/electronics9091493.

[14] F. Yucel and E. Yuce, "Supplementary CCII based second-order universal filter and quadrature oscillators", *AEU - International Journal of Electronics and Communications*, vol. 118, p. 153138, 2020. DOI: 10.1016/j.aeue.2020.153138.

[15] S.-F. Wang, H.-P. Chen, Y. Ku, and C.-M. Yang, "Independently tunable voltage-mode OTA-C biquadratic filter with five inputs and three outputs and its fully-uncoupled quadrature sinusoidal oscillator application", *AEU - International Journal of Electronics and Communications*, vol. 110, p. 152822, 2019. DOI: 10.1016/j.aeue.2019.152822.

[16] S.-F. Wang, H.-P. Chen, Y. S. Ku, and Y.-C. Lin, "Versatile tunable voltage-mode biquadratic filter and its application in quadrature oscillator", *Sensors*, vol. 19, no. 10, p. 2349, 2019. DOI: 10.3390/s19102349.

[17] S.-F. Wang, H.-P. Chen, Y. Ku, and P.-Y. Chen, "A CFOA-based voltage-mode multifunction biquadratic filter and a quadrature oscillator using the CFOA-based biquadratic filter", *Applied Sciences*, vol. 9, no. 11, p. 2304, 2019. DOI: 10.3390/app9112304.

[18] A. Ranjan, S. Perumalla, R. Kumar, V. John, and S. Yumnam, "Second order universal filter using four terminal floating nullor (FTFN)", *Journal of Circuits, Systems and Computers*, vol. 28, no. 6, 2019. DOI: 10.1142/S0218126619500919.

[19] R. Sotner, O. Domansky, J. Jerabek, N. Herencsar, J. Petrzela, and D. Andriukaitis, "Integer-and Fractional-Order Integral and Derivative Two-Port Summations: Practical Design Considerations," *Applied Sciences*, vol. 10, no. 1, p. 54, Dec. 2019. DOI: 10.3390/app10010054.